Curdione induces G2/M phage arrest, apoptosis and autophagy via COX2 mediate IDO1 expression through PKCδ/ GSK3β/β-catenin pathway in human uterine leiomyosarcoma

Chao wei
Capital Medical University
Donghua Li (lidh320@163.com)
Capital Medical University https://orcid.org/0000-0002-7532-9754
Wenna Wang
Capital Medical University
yu Liu
Capital Medical University
tiantian Qiu
Capital Medical University

Research

Keywords: Curdione, apoptosis, autophagy, human uterine leiomyosarcoma

Posted Date: August 26th, 2020

DOI: https://doi.org/10.21203/rs.3.rs-63541/v1

Abstract

Background Curdione, one of active ingredients of a traditional Chinese herb medicine-Curcuma zedoary, has been reported with beneficial therapeutic effects in lots of cancer types. However, the potential anti-cancer effect in uterine leiomyosarcoma (uLMS) and the underlying mechanisms are still unclear.

Methods The aim of this study was to explore the potential effect and mechanisms of curdione on uLMS in vitro and vivo with uLMS cell lines and mouse xenograft tumor model respectively.

Results Curdione triggered anti-proliferation effect in uLMS cell lines by inducing cell cycle arrest at G2/M phase, caspase-mediated cell apoptosis, and pro-death cell autophagy. Indoleamine-2,3-dioxygenase-1 (IDO1), which was dependent on cyclooxygenase-2 (COX2), mediated the anti-proliferation effect of curdione. Curdione down-regulated IDO1 expression and promoted the dephosphorylation of protein kinase c (PKC), glycogen synthase kinase-3 beta (GSK3β) and β-catenin in cell lines. PKC/GSK3β/β-catenin pathway responsible for constitutive IDO1 expression in uLMS. COX2 mediate the promotion effect of curdione on the PKC/GSK3β/β catenin pathway activity, which was detected by COX2 inhibitor, and further confirmed by COX2 siRNA and COX2 overexpression. The pathway activity was inhibited by COX2-siRNA and enhanced by COX2 overexpression. In turn, the pathway inhibitor suppressed IDO1 expression. The anti-proliferation effect of curdione on uterine leiomyosarcoma were further confirmed in vivo. Echoing to the results in vitro, the underline mechanism involved in COX2-mediated IDO1 down-regulation via PKCδ/GSK3β/β-catenin pathway.

Conclusion COX2-mediated IDO1 down-regulation via PKCδ/GSK3β/β-catenin pathway involved in the anti-proliferation effect of curdione on uterine leiomyosarcoma in vitro and vivo.

Background

Uterine leiomyosarcoma is a rare aggressive gynecologic malignancy [1, 2], which is characterized by high recurrence rate, distant metastases, low mortality rate, poor prognosis and poor outcome [3–7]. As the most common subtype of uterine sarcoma, uterine leiomyosarcoma is accompanied by clinical presentation: abnormal uterine bleeding, palpable pelvic mass, and lower abdominal pain, which mimics uterine leiomyoma [5, 8, 9], so clinically faced with poor diagnose. To date, no standardized therapy plan has been made for uLMS because of its rarity and rapid progression. Efforts are currently underway to explore effective therapy strategy.

Accumulating evidences identified that, tumor progression is close relate to proliferation, cell cycle, apoptosis and autophagy. Cell cycle is associate with the cell proliferation and death, and often used as indicator of the antitumor drugs. Here, flow cytometry were performed to detect the effects of curdione on the cell cycle progression. Apoptosis is a form of programmed cell death, which is characterized by TUNEL and PI staining positive. Apoptotic program is mediated by two major pathways–intrinsic and extrinsic pathways apoptotic [10, 11]. Hypoxia, chemotherapy and radiation induce intrinsic pathway in mitochondria [12]. To detect the pathway mediate apoptosis cell death of uLMS induced by curdione,

flow cytometry and western blot analysis were performed to evaluate the expression of apoptosis-related proteins.

As an important indicator of cellular fate, autophagy play a double role in the development of tumor [13, 14]. The LC3-II level is positively relate to the formation of autophagosomes [15].

Sequestosome1 (SQSTM1/P62), which is highly down-regulated when autophagy occur, participated in autophagic degradation, and often used as a marker of autophagy [16]. Beclin-1 also participated in physiological processes of autophagy, and the protein expression level is positive relate to autophagy [17]. We wondered whether curdione induced autophagy in uLMS cells, the level of autophagic relate marker proteins LC3-II, Beclin-1 and P62 were determined by western blot.

IDO1, which plays an important role in promoting the growth of cancers, is over-express in many cancer types and predicts poor outcome [9]. Growing evidence suggest that IDO1 contribute to cancer development [18]. Furthermore, lots of antitumor drugs induced apoptosis and autophagy via declining IDO1 levels in cancers [19, 20]. Accordingly, decreasing IDO1 expression is a key to explore new anticancer drugs. COX-2 is highly expressed in many cancer types and is associate with cancer progression [21, 22]. Considerable evidences suggest that blocking of COX-2 expression could inhibited tumor progression effectively [23–25].

For time immemorial, Chinese herb medicine play a pivotal role in the history of human fighting against diseases. In clinical practice reports of traditional Chinese medicine, herbs or the extractions show widely antibacterial, anti-inflammatory and anticancer efficacy with tolerable toxicity. Therefore, the development of anticancer drugs was refocused on herb medicine. *Rhizoma Curcuma* has been reported with anti-tumor effect [26], which mainly dependent on its essential oils. The effective bioactive compounds of the essential oils including: β-elemene, curcumol, curcumin, curdione, furanodiene, furanodienone, and germacrone have been reported with anti-platelet aggregation [27, 28], anti-inflammatory [29], antibacterial [30], neuroprotective properties [31], prevent cardiotoxicity [32], and anti-tumor effect [26, 30, 33–36]. Beneficial therapeutic effect of curdione has been reported in breast cancers [34], but the potential anti-cancer effect in uLMS and the underlying mechanism is still unclear.

In this paper, we hypothesized that curdione might be one of the effective active components responsible for the anti-tumor effect. The anti-tumor effect of curdione on uLMS was explored by SK-UT-1 and SK-LMS-1 cells in vitro and SK-UT-1 xenograft mice mode in vivo. Cell Counting Kit-8 (CCK-8) assay, immunofluorescence for 5-ethynyl-2'-deoxyuridine (EdU) and Terminal deoxynucleotidyl transferase–mediated dUTP nick-end labeling (TUNEL) assay, flow cytometry, immunohistochemistry, Transient transfection, quantitative real-time reverse transcription-polymerase chain reaction (qRT-PCR), and western blot analysis were conducted to detect the effect of curdione on uLMS, and further elucidate the mechanism.

Materials And Methods

Reagents Curdione purchased from Solarbio Science&Technology Co., Ltd (Beijing, China). IDO1 inhibitor epacadostat purchased from selleck, Modified Eagle's medium (MEM), Dulbecco's modified Eagle's medium (DMEM), Fetal bovine serum (FBS), Non-Essential Amino Acids (NEAA), Pymvate Sodium (NaP), and penicillin-streptomycin (PS) were purchased from Gibco (Waltham, MA, USA). Cell counting kit-8 kit (CCk8) purchased from Dojindo (Kumamoto, Japan). Beyo ClickTM EdU-594 Cell Proliferation Kit purchased from Beyotime (Shanghai, China). Annexin V-fluorescein isothiocyanate (FITC) cell apoptosis kit purchased from Invitrogen. Cell culture SK-UT-1 and SK-LMS-1 cells were obtained from American Type Culture Collection (Manassas, VA, USA). SK-UT-1 cells were cultured in MEM, supplemented with 10% FBS, 1% NEAA, 1% NaP, and 1% penicillin-streptomycin. SK-LMS-1 cells were grown in DMEM supplemented with 10% FBS and 1% penicillin-streptomycin. Both cell lines were incubated in a humidified atmosphere with 5% CO2 at 37°C. Cell viability assay The cell viability detection was performed using the CCK-8 kit. SK-UT-1 and SK-LMS-1 cells were starved with serum-free medium, and then, incubated with gradient concentrations of curdione for 24 h, or with 100 μM curdione for 24, 48 and 72 h; in another experiment, starved cells were pre-treated with IDO1 inhibitor Eapacadostat, autophagy inhibitor 3-Methyladenine (3-MA), GSK3β inhibitor Rottlerin, β-catenin inhibitor LY2090314, COX2 inhibitor NS-398 for 2 h, and then, with curdione or not for 24 h. 10 μl/well CCK8 solution were added into cells and incubated at 37 °C for 2 h, the 450nm OD values were detected at a microplate spectrophotometer (BioTek, USA). Immunofluorescence The proliferation effect of curdione on SK-UT-1 and SK-LMS-1 cell was determined by EdU assay and Ki67 expression. EdU assay were performed using Beyo ClickTM EdU-594 Cell Proliferation Kit (Beyotime) according to the manufacturer's instructions. Simply, after treatment with curdione, cells were incubated with EdU, and then, fixed with 4% paraformaldehyde and permeabilized with 0.3% Triton X-100. After further incubation with Click additive solution, nucleus were stained with Hoechst33342. The proliferation marker Ki67 expression levels in both cell lines were detected by incubation with the primary antibody against Ki67 (ab15580, Abcam, Cambridge, UK), followed with fluorophore-conjugated secondary antibody for 1 h, the nucleus were stained with 4,6-diamino-2-phenyl indole (DAPI, Genview, Florida, USA). For TUNEL assay, according to the manufacture's protocols of TUNEL assay kit (KeyGen, Nanjing, China). Cells were stained with TUNEL, Laser confocal microscope (Leica DM60008, Kyoto, Japan) was used to detect the stained-positive expression levels. The number of EdU, Ki67 and TUNEL positive cells from six random fields were used for quantitatively analysis using Image J software. Flow cytometry analysis Annexin V- FITC & PI cell apoptosis kit (V13241, Invitrogen, USA) were used to detect cell apoptosis according to instruction. Briefly, starved cells were exposed to curdione for 24 h, or pretreated with pharmaceutical inhibitor for 2 h, following with curdione or not for 24 h, cells were harvested and co-stained with AnnexinV-FITC/PI. For cell cycle analysis, according to the manufacturer's instructions of Cell Cycle and Apoptosis Analysis Kit (Beyotime, Shanghai, China), cells were fixed with 70% cold ethanol for 24 h, and then, incubated with 5 μl PI staining and 45 μl RNase water. Subsequently, all prepared samples were analyzed by flow cytometry (BD Biosciences, San Jose, CA, USA). Transient transfection Specific siRNA target COX2 and IDO1 were designed and synthesized by RiboBio Co, Ltd (Beijing, China) respectively. The SK-UT-1 and SK-LMS-1 cells were transfected according to the manual. The siRNA sequence targeting IDO1 (5 '-GGATGTTCATTGCTAAACA -3 '), COX2 (5 '- TAAGTGCGATTGTACCCGGAC - 3 '); human COX2 and IDO1

overexpression vector were constructed by RiboBio Co, Ltd, and the transfection protocol according to the manufacturer instruction. The protein and mRNA expression levels were further confirmed 24 h later. Western blot assay The total protein from tissues or cells were extracted, and then, quantified by the BCA Protein Assay kit (Beyotime, Shanghai, China). Equal proteins (30 μg) from each sample were separated by SDS-PAGE (Solarbio, Beijing, China) and then, transferred to polyvinylidene fluoride microporous membranes (PVDF) (Millipore, MA, USA), the membranes were blocked and incubated with primary antibodies against: IDO1 (ab211017, Abcam), COX2 (ab179800, Abcam), caspase-3 (ab13847, Abcam) , cleaved-caspase-3 (ab2302, Abcam), caspase-6 (ab185645, Abcam), cleaved-caspase-6 (ab2326, Abcam), caspase-9 (ab32539, Abcam), cleaved-caspase-9 (ab2324, Abcam), caspase-8 (ab108333, Abcam), Cleaved-caspase-8 (9496, Cell Signaling), LC3 (ab48394, Abcam), Beclin1 (ab210498, Abcam), P62 (ab109012, Abcam), p-GSK-3β (Ser9) (ab75814, Abcam), GSK-3β (ab3239, Abcam), PKCδ (ab59364, Abcam), p-PKCδ (ab59412, Abcam) β-catenin (ab16051, Abcam), p-β-catenin (Ser552)(9566, Cell Signaling), GAPDH (ab181602, Abcam). Followed by HRP-conjugated secondary antibody with corresponding peroxidase. Enhanced Chemiluminescence (ECL) detection kit (Thermo Scientific, Waltham, MA, USA) was used to visual the immunoblot signals on an imaging system (Bio-Rad, USA). The results were analyzed using Image J software. The relative protein expressions of IDO1 and COX-2 were normalized to that of GAPDH, respectively. The phosphorylation proteins were normalized to the corresponding total protein. Quantitative real-time RT-PCR Total RNA extraction, cDNA synthesis and RT-PCR were performed respectively using ES- science RNA-Quick Purification Kit、Fast All-in-One RT Kit and 2xSuper SYBR Green qPCR Master Mix (YiShan Biotech, Shanghai, China) according to the protocol. Real-time PCR was conducted on the ABI-7500 Sequence Detection System (Applied Biosystems, Foster City, CA, USA) according to the program: pre-incubation 95°C 5 min, followed by 40 cycles of denaturation 95 °C 10 s, annealing 60°C 1 min, and 60°C 30 s extension. The relative mRNA levels of IDO1 and COX2 were normalized to GAPDH. The comparative cycle threshold (Ct) method ($2^{-\Delta\Delta CT}$) was used to calculate the fold change of RNAs expression. Independent experiments repeat three times. The primer sequences were present: IDO1 (F: GCCAGCTTCGAGAAAGAGTTG R: ATCCCAGAACTAGACGTGCAA) COX2 (F: CTGGCGCTCAGCCATACAG R: CGCACTTA TACTGGTCAAATCC). GAPDH (F: GGAGCGAGATCCCTCCAAAAT R: GGCTGTTGTCA TACTTCTCATGG) Mouse xenograft tumor model 6–8 weeks female nude mice (18 ± 2 g) purchased from Beijing Vital River Laboratory Animal Technology (Beijing, China). Approximately 1×107 SK-UT-1 cells were suspended and injected subcutaneously into the right flank of nude mice. When the tumors volume reached approximately 50 mm3, the mice were randomly divided into three groups (n = 5), mice were injected intraperitoneal (i.p) with 100 or 200 mg/ kg curdione or same volume saline every day. After 21 days, all mice were sacrificed, the tumor weight and volume, mice weight were determined, and the tumors tissue were collected for immunhistochemical staining and western blot analysis at indicated time point. All experimental protocols performed in accordance with the Guidelines for the Care and Use of Laboratory Animals by the National Institute of Health, and approved by the Ethics Committee of Capital Medical University. Histopathology and immunohistochemistry Tissues of tumor, liver and kidney were harvest and embedded in 4% paraformaldehyde, and then, tissues were stained with hematoxylin and eosin (H&E), the tumor tissues were incubated with primary antibodies overnight. Images were captured by a light microscopy (Leica

DM60008, Kyoto, Japan). Statistical analysis Data are present as mean ± SD of three independent experiments. Statistical analysis were performed using SPSS version 19.0 software (SPSS Inc., IL, USA), One-way analysis of variance ANOVA was used for compare analysis the significant differences among groups by student's unpaired t test. $P<0.05$ were considered statistically significant.

Results

Curdione suppresses human uterine leiomyosarcoma cells viability

After treatment with grade concentrations (0-500 μM) *curdione* for 12, 24, 48 and 72 h, the SK-UT-1 and SK-LMS-1 cells viability were detected by CCK8 assay respectively. As shown in Fig. 2, curdione inhibited the cells viability in a concentration and time dependent manner at concentration higher than 10 μM. The 50% inhibited concentration (IC50) were determined to find the ideal dose for the following experiments. The IC50 and the corresponding 95% confidence intervals of SK-UT-1 and SK-LMS-1 cell are 327.0 (297.7 -362.8) μM and 334.3 (309.9 - 362.5) μM respectively. To ensure more than 85% cells under good condition for following experiments, less than one third of IC50 curdione (100 μM) for proper dose.

Curdione inhibited human uterine leiomyosarcoma cells proliferation

To further confirm the anti-proliferation effect of Curdione on uterine leiomyosarcoma cell, SK-UT-1 and SK-LMS-1 cells were treated with curdione for 24 h, EdU assay and the proliferation marker ki67 were detected by immunofluoresent. As Fig.3 shows, compared with control, curdione decreased the EdU and ki67 positive rate of both cell lines in a concentration dependent manner.

Curdione induces G2/M phase arrest in human uterine leiomyosarcoma cells

There are close relation between proliferation and cell cycle distribution. To explore the effect of curdione on cell cycle progression, flow cytometry analysis was conducted to detect the cycle distribution, western blot were conducted to detect the cell cycle related proteins. As shown in Fig 4 **a**, compared with control the G2/M population increased after treated with 100 μM Curdione for 24 h, The cell populations in S phase decreased, and no significant changes occur in G0/G1 phase. Which indicated that, curdione induced cell cycle arrest in G2/M phase. The cell cycle related proteins analysis show that, curdione up-regulated the proteins P21 and CyclinB1, while down regulated Cdc2.

Curdione induces apoptosis in human uterine leiomyosarcoma cells

Curdione induced both early and late apoptotic of cells in a concentration-dependent manner. After treatment with curdione or not for 24 h, flow cytometry was performed with Annexin V-FITC/ Propidium Iodide (PI) double staining to quantify apoptosis. As shown in Fig.5, compared with control, the early apoptotic ratio elevated by 2.95-fold (1.9% and 1.6%) and 4.25-fold (5.6% and 6.8%) respectively; the late apoptotic ratio increased from 1.9% to 6.4% in SK-UT-1 cells, and from 1.2% to 4.9%in SK-LMS-1 cells; the

total apoptosis ratio increased by 8.2% in SK-UT-1, and 8.9% in SK-LMS-1 cells. Which indicated that, both early and late apoptotic ratio of SK-UT-1 and SK-LMS-1 cells increased with curdione treatment in a dose-dependent manner.

Curdione induces autophagy in human uterine leiomyosarcoma cells

Autophagy is another important mechanism that regulate cell fate. To detect whether autophagy was induced by curdione, the level of autophagic marker proteins LC3-II, Beclin-1 and P62 in both cells were determined by western blotting. As shown in fig 6, curdione upregulated LC3-II and Beclin-1, and downregulated P62 in a dose-dependent manner. To further clarify that autophagy induced by curdione was pro-survival or pro-death, 3-MA (an autophagy inhibitor) was used to detect the influence of cell viability. Before treated with curdione, SK-UT-1 and SK-LMS-1 cells were incubated with autophagy inhibitor 3-MA for 2 h, the results showed that, 3-MA blocked the inhibitory effect of curdione on cell viability and apoptosis of SK-UT-1 and SK-LMS-1 cells significantly.

Curdione induced the crosstalk between apoptosis and autophagy in human uterine leiomyosarcoma cells

Curdione induced apoptosis and autophagy, to explore whether there was crosstalk between apoptosis and autophagy. SK-UT-1 and SK-LMS-1 were pre-treatment with Z-VAD-FMK (apoptosis inhibitor) or 3-MA (autophagy inhibitor) for 2 h, and then incubated with curdione for 24 h, apoptosis ratio were detected by flow cytometry. The apoptosis and autophagy marker proteins were determined by western blot. The results showed that, apoptosis ratio induced by curdione was blocked by Z-VAD-FMK and abolished by 3-MA (Fig.7 **a**). Western blot results show that, the decreased expression of LC3II, beclin1 and increased expression of p62 induced by curdione were alleviated by Z-VAD-FMK, the up regulation of cleaved caspase 3, 6, 9 induced by curdione were attenuated by 3-MA (Fig.7 **b**).

Curdione inhibited IDO1 expression in human uterine leiomyosarcoma cells

Western blot were performed to quantify the effect of curdione on IDO1 protein expression in SK-UT-1 and SK-LMS-1 cells. As Fig. 8 shows, Curdione down-regulated IDO1 expression of human uterine leiomyosarcoma cells in a concentration – dependent manner. The above data show that, curdione suppressed the proliferation of SK-UT-1 and SK-LMS-1 cells and down-regulated IDO1 expression. To further detected the relationship between regulation effect on IDO1 expression and anti-proliferation of curdione in both cell lines. Cells were pretreatment with IDO1 inhibitor for 2 h, and then incubated with curdione for 24 h. The results showed that, epacadostat reversed the suppression effect on cell viability induced by curdione in both cell lines. To further investigate this effect, IDO1 knockdown and overexpression were performed. The results showed that, compared with curdione alone group, silence of

IDO1 overcame the suppression effect on cell viability induced by curdione. While, IDO1 overexpression enhanced the inhibitory effect induced by curdione.

COX2 is necessary for curdione-decreased IDO1 expression in human uterine leiomyosarcoma cells

To explore whether IDO1 mediate the suppression effect of curdione is dependent on COX2. NS398, an antagonism of COX2, significantly reversed the inhibitory effect of curdione on IDO1 expression in SK-UT-1 and SK-LMS-1 cells. To further confirm that, COX2 mediates curdione down-regulated IDO1 expression, transiently transfection technology approaches to manipulate COX2 expression in both cell lines were designed. Silence or overexpression of COX2 in mRNA and protein levels were confirmed by qRT-PCR and western blot analysis, knockdown COX2 reversed the inhibitory effect of curdione on IDO1 expression, while the inhibitory effect significantly enhanced by the over expression of COX2 in both cell lines. These findings collectively indicated that, dependent on COX2, curdione suppressed IDO1 expression in SK-UT-1 and SK-LMS-1 cells.

PKCδ/GSK3β/β-catenin pathway mediate curdione decrease IDO1 expression in uLMS cells

To further illustrate the mechanism involved in COX2-mediated induction of IDO1 expression in uLMS. The effects of curdione on the activation of PKCδ, GSK3β and β-catenin in human uterine leiomyosarcoma cells were detected. As shown in Fig 10, curdione promoted the PKCδ, GSK3β and β-cantein dephosphorylation significantly in a concentration-dependent manner. COX2 antagonist NS398 blocked the dephosphorylation of PKCδ, GSK3β and β-catenin pathway. To further confirm this mechanism, SK-UT-1 and SK-LMS-1 cells were transfected with either COX2-siRNA or COX2-pCMV6, and then treated with curdione for 24 h. The results show that, the PKCδ, GSK3β and β-catenin pathway activation were attenuated by COX2-siRNA and enhanced by the overexpression of COX2. The PKCδ, GSK3β and β-catenin pathway activity and the inhibitory effect of curdione on IDO1 expression were abolished by PKCδ inhibitor and GSK3β inhibitor. Which indicated that, the depression effect of curdione on IDO1 expression is mediated by the dephosphorylation of the PKCδ, GSK3β and β-catenin pathways in uLMS cells.

Curdione inhibited cell proliferation by induced cell cycle arrest in G2/M, apoptosis and autophagy in human uterine leiomyosarcoma cells

To confirm whether downregulation IDO1 is involved in the anti-proliferation of curdione in uLMS cells and mediated by the PKCδ/GSK3β/βcatenin dependent COX-2 pathway, SK-UT-1 and SK-LMS-1 cells were pretreatment with rottlerin or LY2090314 or NS398 for 2 h, and then incubated with curdione for 24 h. As shown in Fig. 11**a**, the anti-proliferation effect of curdione was attenuate by selective GSK3β inhibitor Rottlerin and β catenin inhibitor LY2090314, and COX-2 inhibitor NS-398 blocked the anti-proliferation effect of curdione. Fig. 11**b** shows that, the upregulation of cleaved-caspase 3, LC3, Beclin1, Cdc2, CyclinB1 and down regulation of P62 induced by curdione were abolished by IDO1 inhibitor epacadostat, GSK3β inhibitor Rottlerin, β catenin inhibitor LY2090314 and COX-2 inhibitor NS-398. The above results

collectively indicated that IDO1 mediated PKCδ/GSK3β/βcatenin pathway dependent on COX-2 is involved in the anti-proliferative effect of curdione on human uterine leimyosarcoma cells.

Curdione suppress the growth of uterine leiomyosarcoma in vivo

To further explore the anti-uterine leiomyosarcoma effect of curdione in vivo, we established a xenograft tumor model by subcutaneous injection with SK-UT-1 cells into the right flanks of BALB/c nude mice. Tumor xenograft mice were intraperitoneal injection with 100 mg/kg/day or 200 mg/kg/day curdione or not for 21 days. The body weight, histopathological examination, tumor volume and weight were measured to evaluate the effect of curdione on the uterine leiomyosarcoma in vivo. Fig. 12 **a-e** showed that, compared with control, curdione reduced tumor volume and weight markedly. While, no significant body weight loss were detected in curdione treated xenograft mice. The histopathological results showed that, no obvious histopathological lesion were detected in liver and kidney tissue, which meaning curdione induced no liver and kidney injuries in vivo (Fig. 8 **f**). Above all, Curdione exhibited anti-uterine leiomyosarcoma efficacy with few toxicity in vivo.

Curdione induces apoptosis and autophagy in SK-UT-1 xenografts

To determine the mechanism involved in the inhibitory effect of curdione on human uterine leiomyosarcoma *in vivo.* The tissues protein expression of IDO1, COX2, the cleaved caspase-3, LC3-II, Becline1, P62, PKCδ, GSK3β, β-catenin were detected by western blot and immunohistochemistry assay. Consistent with the results in vitro, curdione up-regulated the protein expression of IDO1, COX2, the cleaved caspase-3, LC3-II, dephosphorylation of PKCδ, GSK3β, β-catenin and down-regulated ki67, p62 in tumor tissues (Fig. 13 **a**). The immunohistochemistry assay showed the same changes of protein levels observed in western blot (Fig. 13 **b**). The above results showed that, echoing to the results in vitro, curdione inhibited the expression of IDO1, COX2 and the phosphorylation of PKCδ/GSK3β/β-catenin pathway in vivo. In conclusion, acting on COX2 mediate IDO1 expression via PKCδ, GSK3β, β-catenin pathway, curdione suppress the growth of human uterine leiomyosarcoma in tumor xenografts.

Discussion

ULMS is a highly malignant tumor with poor outcome (low five-year survival rate and high recurrence rate) [37]. To date, no safe and effective medications for uterine leiomyosarcoma have been developed [38, 39], it is imperative to find effective medicine for this disease.

With the effect of promoting blood circulation, removing blood stasis and alleviating pain, *Rhizoma Curcumae* has been widely prescribed for the treatment of gynecological diseases in Traditional Chinese Medicine clinical practice. Mounting studies have shown that, the *Rhizoma Curcumae* extracts, which have broad-spectrum antitumor effects, play an important role in the effect of herb medicine. Curcumin, which comes from the same family and genus with curdione, has the anti-proliferation effect on uterine sarcoma [36, 40]. As one of the extracts of *Rhizoma Curcumae*, curdione have the same chemical structure with curcumin, so we speculate that curdione has similar anti-tumor effect on uLMS.

In this work, we determined the effect of curdione on the cells viability. The results as Fig. 2 showed that, in a dose and time dependent manner, curdione inhibited the viability of SK-UT-1 and SK-LMS-1 cells. To ensure the fidelity and reliability, less than a third of IC50 were used as the optimal dose in the following experiment. The anti-proliferation effect of curdione were further confirmed by EdU assay, which often used to reflect the DNA replication activity indirectly, and ki67 expression levels, a marker of proliferation, which was detected by immune florescence. As shown in Fig. 3, curdione suppressed EdU-positive and Ki67-positive florescence images in a dose dependent manner in both cell lines. Cell cycle, which is close related to cell fate, is often used to evaluate the efficacy of new drugs. In this study, curdione increased the cells population of G2/M phase in a concentration dependent manner in uLMS cell lines.

Apoptosis is a form of programmed cell death, also an important mechanism of cellular self-protective. Here, curdione induced SK-LMS-1 and SK-UT-1 cells pro-death apoptosis in a dose-dependent manner, the apoptosis ratio were detected by flow cytometry analysis with Annexin V-FITC/PI double staining, and the apoptosis morphology changes were determined by TUNEL analysis. Li reported that β-elemene induced caspase-mediated mitochondrial cell apoptotic [41]. Similarly, western blot analysis show that, the proteins expression levels of cleaved caspase3, 6, 9 increased in a dose-dependent manner, while no changes occur in pro- and cleaved-caspase 8 (Fig. 4), which suggest that, curdione induced caspase-mediated apoptosis through intrinsic pathway.

Autophagy, just like a double edged sward–pro-survival or pro-death, is also another important mechanism that regulate the behavior of tumor. Here, as shown in Fig. 5, curdione induce autophagy, which were reflect by the increased LC3-II, Beclin-1 expression and down regulated P62 expression. To further clarify the autophagy induced by curdione was pro-survival or pro-death. The cell viability were detected when cells were pretreated with 3-MA (autophagy inhibitor) followed by curdione. 3-MA blocked inhibitory effect of curdione on cell viability. The results indicated that, curdione induced pro-death autophagy in SK-UT-1 and SK-LMS-1 cells. Based on these data, we demonstrated that, curdione inhibited the growth of uLMS by inducing cell cycle arrest, apoptosis and autophagy in SK-UT-1 and SK-LMS-1 cells.

IDO1, which play an important role in the cancer development [42], is highly expressed in many cancer types [43–45]. High IDO1 expression is associated with poor overall survival and progression-free survival [46–49]. According to Liu report, compared with paired normal tissues, IDO1 is highly expressed in uterine carcinosarcoma and uterine corpus endometrial carcinoma [46], but the expression level in uterine leiomyosarcoma is still unclear. In the pre-trail, we found high IDO1 expression in SK-UT-1 and SK-LMS-1 cells. Here, the inhibitory effect of curdione on IDO1 expression were determined, and further, we analyzed the correlation between IDO1 expression and the anti-proliferation effect of curdione, as shown in Fig. 5. The inhibitor of IDO1 reversed the suppression effect of curdione on uLMS cell lines significantly, and the suppression effect were overcame by silence of IDO1, while enhanced by IDO1 overexpression. These data indicated that the suppression effect of curdione on the growth of uLMS is mediated by IDO1.

As one of the immune checkpoints, IDO1 participated in limiting immune surveillance, promoting tumor immune tolerance and immune escape [46, 50, 51]. As a “brake” or “accelerator” in the tumor immune regulation, IDO1 prepare immunosuppressive tumor microenvironment [52]. However, Ameet I. Thaker reported that, independent on T cell mediated immune regulation, IDO1 induce colon cancer growth directly [42]. In this work, we found that, IDO1 mediated the anti-proliferative effect of curdione in uLMS. Further research is need to analysis whether this effect dependent on IDO1 activity mediate immune response, which was detected by analyzing tryptophan levels, kynurenine levels and immune response.

COX-2 was found to be overexpression in primary or metastatic lesions of many tumor types [53]. COX-2 stimulate proliferation, promote angiogenesis, and participate in the tumor occurrence directly [54–56], which indicates that COX-2 regulate tumor biological behavior. COX2 and IDO1 co-expression in many human cancer types [57], according to Zhang et al, COX2 is driver of IDO1 in colon cancer [53]. In the pre-trail, we determined high COX2 expression in both cell lines. We speculate that, COX2 may drive IDO1 expression in SK-UT-1 and SK-LMS-1 cells, in this study, through inhibitor and genetic technology, we further reveal the interactions between COX2 and IDO1 expression in the present of curdione. The results indicated that COX-2 is essential for curdione suppressed IDO1 expression, which is consistent with the results of Cianchi [58].

Previous studies have found that, PKC/GSK3β/βcatenin pathway is a bridge of COX2 triggers IDO1 expression in human cancers [57]. To further explore the signaling pathway responsible for constitutive IDO1 expression in uLMS, the activation of PKC/GSK3β/βcatenin pathway were determined. Curdione promoted the dephosphorylation of the pathway in a concentration dependent manner, this was blocked by COX2 inhibitor NS398, which means that curdione induced the pathway activity is mediated by COX2, this was further confirmed by silence of COX2 and overexpression of COX2. As Fig. 10 shows, the pathway activity was inhibited by COX2-siRNA and enhanced by COX2 overexpression. In turn, the pathway inhibitor suppressed IDO1 expression in both cell lines.

Conclusions

In this paper, for the first time, we demonstrated the anti-tumor effect of curdione on uLMS and analyzed the underlying mechanisms. Curdione induced cell cycle arrest, apoptosis and autophagy, which jointly promote cell death powerful. The crosstalk between apoptosis and autophagy suppressed the progression of uLMS. The mechanisms, which were involved in COX2 mediated IDO1 expression via PKCδ/GSK3β/βcatenin pathway, were explored further by pharmaceutical inhibitor and transfection technology. In addition, the safety of curdione in vivo was checked by detecting the body weight changes of xenograft tumor models and histological analysis of virtual organs - kidney and liver.

Taken together, curdione, extract from natural herb medicine, is a promising candidate for the treatment or assistant treatment of uLMS. Our research provide preclinical evidence for uterine leiomyosarcoma treatment and open a new perspective in the war against uLMS.

Abbreviations

uLMS: uterine leiomyosarcoma; IDO1: Indoleamine-2,3-dioxygenase-1; COX2: cyclooxygenase-2; PKC: protein kinase c; GSK3β: glycogen synthase kinase-3 beta; CCK-8: Cell Counting Kit-8; FITC: Annexin V-fluorescein isothiocyanate; DAPI: 4,6-diamino-2-phenyl indole ; EdU: 5-ethynyl-2'-deoxyuridine; TUNEL: Terminal deoxynucleotidyl transferase–mediated dUTP nick-end labeling; qRT-PCR: quantitative real-time reverse transcription-polymerase chain reaction.

Declarations

Ethics approval and consent to participate

All experimental protocols approved by the Ethics Committee of Capital Medical University.

Consent for publication

All contributing authors agree to the publication of this article.

Availability of data and materials

All data generated or analyzed during this study were included in this published article.

Competing interests

All authors declare no potential competing interests.

Funding

This study was supported by National Natural Science Foundation of China (81774072, 81373812, 81073096) and Natural Science Foundation of Beijing Municipality (7202015)

Authors' contributions

CW is in charge of the whole experiment conduction and paper writing. CW and L-DH designed the original experiments, whereas W-NW, T-TQ and YL helped conduct the experiment and added helps in the experiments. All authors reviewed and approved the final manuscript.

Acknowledgements

Not applicable

References

1. Major FJ, Blessing JA, Silverberg SG, Morrow CP, Creasman WT, Currie JL, et al. Prognostic factors in early-stage uterine sarcoma. A Gynecologic Oncology Group study. Cancer. 1993;71(4 Suppl):1702–9.
2. Skorstad M, Kent A, Lieng M. Uterine leiomyosarcoma - incidence, treatment, and the impact of morcellation. A nationwide cohort study. Acta Obstet Gynecol Scand. 2016;95(9):984–90.

3. Gadducci A, Landoni F, Sartori E, Zola P, Maggino T, Lissoni A, et al. Uterine leiomyosarcoma: analysis of treatment failures and survival. Gynecol Oncol. 1996;62(1):25–32.
4. Seagle BL, Sobecki-Rausch J, Strohl AE, Shilpi A, Grace A, Shahabi S. Prognosis and treatment of uterine leiomyosarcoma: A National Cancer Database study. Gynecol Oncol. 2017;145(1):61–70.
5. Kodama K, Sonoda K, Kijima M, Yamaguchi S, Yagi H, Yasunaga M, et al. Retrospective analysis of treatment and prognosis for uterine leiomyosarcoma: 10-year experience of a single institute. Asia Pac J Clin Oncol. 2020;16(2):e63-e7.
6. Hadoux J, Morice P, Lhomme C, Duvillard P, Balleyguier C, Haie-Meder C, et al. [Uterine leiomyosarcoma: epidemiology, pathology, biology, diagnosis, prognosis and treatment]. Bull Cancer. 2013;100(9):903–15.
7. Bogani G, Cliby WA, Aletti GD. Impact of morcellation on survival outcomes of patients with unexpected uterine leiomyosarcoma: a systematic review and meta-analysis. Gynecol Oncol. 2015;137(1):167–72.
8. Zivanovic O, Jacks LM, Iasonos A, Leitao MM Jr, Soslow RA, Veras E, et al. A nomogram to predict postresection 5-year overall survival for patients with uterine leiomyosarcoma. Cancer. 2012;118(3):660–9.
9. Prendergast GC, Smith C, Thomas S, Mandik-Nayak L, Laury-Kleintop L, Metz R, et al. Indoleamine 2,3-dioxygenase pathways of pathogenic inflammation and immune escape in cancer. Cancer Immunol Immunother. 2014;63(7):721–35.
10. Zhao Y, Li R, Xia W, Neuzil J, Lu Y, Zhang H, et al. Bid integrates intrinsic and extrinsic signaling in apoptosis induced by alpha-tocopheryl succinate in human gastric carcinoma cells. Cancer Lett. 2010;288(1):42–9.
11. Midgley A, Mayer K, Edwards SW, Beresford MW. Differential expression of factors involved in the intrinsic and extrinsic apoptotic pathways in juvenile systemic lupus erythematosus. Lupus. 2011;20(1):71–9.
12. Lockshin RA, Zakeri Z. Cell death in health and disease. J Cell Mol Med. 2007;11(6):1214–24.
13. Guo JY, Xia B, White E. Autophagy-mediated tumor promotion. Cell. 2013;155(6):1216–9.
14. Eskelinen EL. The dual role of autophagy in cancer. Curr Opin Pharmacol. 2011;11(4):294–300.
15. Mizushima N, Yoshimori T, Levine B. Methods in mammalian autophagy research. Cell. 2010;140(3):313–26.
16. Sahani MH, Itakura E, Mizushima N. Expression of the autophagy substrate SQSTM1/p62 is restored during prolonged starvation depending on transcriptional upregulation and autophagy-derived amino acids. Autophagy. 2014;10(3):431–41.
17. Kang R, Zeh HJ, Lotze MT, Tang D. The Beclin 1 network regulates autophagy and apoptosis. Cell Death Differ. 2011;18(4):571–80.
18. Wei L, Zhu S, Li M, Li F, Wei F, Liu J, et al. High Indoleamine 2,3-Dioxygenase Is Correlated With Microvessel Density and Worse Prognosis in Breast Cancer. Front Immunol. 2018;9:724.

19. Bishnupuri KS, Alvarado DM, Khouri AN, Shabsovich M, Chen B, Dieckgraefe BK, et al. IDO1 and Kynurenine Pathway Metabolites Activate PI3K-Akt Signaling in the Neoplastic Colon Epithelium to Promote Cancer Cell Proliferation and Inhibit Apoptosis. Cancer Res. 2019;79(6):1138–50.
20. Hascitha J, Priya R, Jayavelu S, Dhandapani H, Selvaluxmy G, Sunder Singh S, et al. Analysis of Kynurenine/Tryptophan ratio and expression of IDO1 and 2 mRNA in tumour tissue of cervical cancer patients. Clin Biochem. 2016;49(12):919–24.
21. Chun KS, Surh YJ. Signal transduction pathways regulating cyclooxygenase-2 expression: potential molecular targets for chemoprevention. Biochem Pharmacol. 2004;68(6):1089–100.
22. Hashemi Goradel N, Najafi M, Salehi E, Farhood B, Mortezaee K. Cyclooxygenase-2 in cancer: A review. J Cell Physiol. 2019;234(5):5683–99.
23. Manvar D, Pelliccia S, La Regina G, Famiglini V, Coluccia A, Ruggieri A, et al. New 1-phenyl-5-(1H-pyrrol-1-yl)-1H-pyrazole-3-carboxamides inhibit hepatitis C virus replication via suppression of cyclooxygenase-2. Eur J Med Chem. 2015;90:497–506.
24. Lin W, Li Z. Blueberries inhibit cyclooxygenase-1 and cyclooxygenase-2 activity in human epithelial ovarian cancer. Oncol Lett. 2017;13(6):4897–904.
25. Shao Y, Li P, Zhu ST, Yue JP, Ji XJ, Ma D, et al. MiR-26a and miR-144 inhibit proliferation and metastasis of esophageal squamous cell cancer by inhibiting cyclooxygenase-2. Oncotarget. 2016;7(12):15173–86.
26. Zhong Z, Chen X, Tan W, Xu Z, Zhou K, Wu T, et al. Germacrone inhibits the proliferation of breast cancer cell lines by inducing cell cycle arrest and promoting apoptosis. Eur J Pharmacol. 2011;667(1–3):50–5.
27. Xia Q, Wang X, Xu DJ, Chen XH, Chen FH. Inhibition of platelet aggregation by curdione from Curcuma wenyujin essential Oil. Thromb Res. 2012;130(3):409–14.
28. Fang H, Gao B, Zhao Y, Fang X, Bian M, Xia Q. Curdione inhibits thrombin-induced platelet aggregation via regulating the AMP-activated protein kinase-vinculin/talin-integrin alphaIIbbeta3 sign pathway. Phytomedicine. 2019;61:152859.
29. Oh OJ, Min HY, Lee SK. Inhibition of inducible prostaglandin E2 production and cyclooxygenase-2 expression by curdione from Curcuma zedoaria. Arch Pharm Res. 2007;30(10):1236–9.
30. Chen C, Long L, Zhang F, Chen Q, Chen C, Yu X, et al. Antifungal activity, main active components and mechanism of Curcuma longa extract against Fusarium graminearum. PLoS One. 2018;13(3):e0194284.
31. Li XJ, Liang L, Shi HX, Sun XP, Wang J, Zhang LS. Neuroprotective effects of curdione against focal cerebral ischemia reperfusion injury in rats. Neuropsychiatr Dis Treat. 2017;13:1733–40.
32. Wu Z, Zai W, Chen W, Han Y, Jin X, Liu H. Curdione Ameliorated Doxorubicin-Induced Cardiotoxicity Through Suppressing Oxidative Stress and Activating Nrf2/HO-1 Pathway. J Cardiovasc Pharmacol. 2019;74(2):118–27.
33. Lu JJ, Dang YY, Huang M, Xu WS, Chen XP, Wang YT. Anti-cancer properties of terpenoids isolated from Rhizoma Curcumae–a review. J Ethnopharmacol. 2012;2(2):406–11.

34. Li J, Bian WH, Wan J, Zhou J, Lin Y, Wang JR, et al. Curdione inhibits proliferation of MCF-7 cells by inducing apoptosis. Asian Pac J Cancer Prev. 2014;15(22):9997–10001.
35. Lu JJ, Dang YY, Huang M, Xu WS, Chen XP, Wang YT. Anti-cancer properties of terpenoids isolated from Rhizoma Curcumae–a review. J Ethnopharmacol. 2012;143(2):406–11.
36. Hashem S, Nisar S, Sageena G, Macha MA, Yadav SK, Krishnankutty R, et al. Therapeutic Effects of Curcumol in Several Diseases; An Overview. Nutr Cancer. 2020:1–15.
37. Juhasz-Boss I, Gabriel L, Bohle RM, Horn LC, Solomayer EF, Breitbach GP. Uterine Leiomyosarcoma. Oncol Res Treat. 2018;41(11):680–6.
38. Roberts ME, Aynardi JT, Chu CS. Uterine leiomyosarcoma: A review of the literature and update on management options. Gynecol Oncol. 2018;151(3):562–72.
39. Ricci S, Stone RL, Fader AN. Uterine leiomyosarcoma: Epidemiology, contemporary treatment strategies and the impact of uterine morcellation. Gynecol Oncol. 2017;145(1):208–16.
40. Ning L, Ma H, Jiang Z, Chen L, Li L, Chen Q, et al. Curcumol Suppresses Breast Cancer Cell Metastasis by Inhibiting MMP-9 Via JNK1/2 and Akt-Dependent NF-kappaB Signaling Pathways. Integr Cancer Ther. 2016;15(2):216–25.
41. Li QQ, Wang G, Huang F, Banda M, Reed E. Antineoplastic effect of beta-elemene on prostate cancer cells and other types of solid tumour cells. J Pharm Pharmacol. 2010;62(8):1018–27.
42. Thaker AI, Rao MS, Bishnupuri KS, Kerr TA, Foster L, Marinshaw JM, et al. IDO1 metabolites activate beta-catenin signaling to promote cancer cell proliferation and colon tumorigenesis in mice. Gastroenterology. 2013;145(2):416–25. e1-4.
43. Kolijn K, Verhoef EI, Smid M, Bottcher R, Jenster GW, Debets R, et al. Epithelial-Mesenchymal Transition in Human Prostate Cancer Demonstrates Enhanced Immune Evasion Marked by IDO1 Expression. Cancer Res. 2018;78(16):4671–9.
44. Schafer CC, Wang Y, Hough KP, Sawant A, Grant SC, Thannickal VJ, et al. Indoleamine 2,3-dioxygenase regulates anti-tumor immunity in lung cancer by metabolic reprogramming of immune cells in the tumor microenvironment. Oncotarget. 2016;7(46):75407–24.
45. Lindstrom V, Aittoniemi J, Jylhava J, Eklund C, Hurme M, Paavonen T, et al. Indoleamine 2,3-dioxygenase activity and expression in patients with chronic lymphocytic leukemia. Clin Lymphoma Myeloma Leuk. 2012;12(5):363–5.
46. Liu M, Wang X, Wang L, Ma X, Gong Z, Zhang S, et al. Targeting the IDO1 pathway in cancer: from bench to bedside. J Hematol Oncol. 2018;11(1):100.
47. Zhu Y, Jiang C, Wu H, Xu Q, Feng J, Xu Y. P2.04-18 The Association Between IDO Activity and Clinical Prognosis in Patients with Non-Small Cell Lung Cancer After Radiotherapy. Journal of Thoracic Oncology. 2018;13(10).
48. <cyclooxygenase-2 and indoleamine 2,3-dioxygenase promotes breast cancer progression.pdf>.
49. Hornyak L, Dobos N, Koncz G, Karanyi Z, Pall D, Szabo Z, et al. The Role of Indoleamine-2,3-Dioxygenase in Cancer Development, Diagnostics, and Therapy. Front Immunol. 2018;9:151.

50. Li F, Zhang R, Li S, Liu J. Corrigendum to "IDO1: An important immunotherapy target in cancer treatment" [Int. Immunopharmacol. 47 (2017) 70–77]. Int Immunopharmacol. 2017;49:231.
51. Vigneron N, van Baren N, Van den Eynde BJ. Expression profile of the human IDO1 protein, a cancer drug target involved in tumoral immune resistance. Oncoimmunology. 2015;4(5):e1003012.
52. Sharma P, Hu-Lieskovan S, Wargo JA, Ribas A. Primary, Adaptive, and Acquired Resistance to Cancer Immunotherapy. Cell. 2017;168(4):707–23.
53. Hennequart M, Pilotte L, Cane S, Hoffmann D, Stroobant V, Plaen E, et al. Constitutive IDO1 Expression in Human Tumors Is Driven by Cyclooxygenase-2 and Mediates Intrinsic Immune Resistance. Cancer Immunol Res. 2017;5(8):695–709.
54. Cai F, Chen M, Zha D, Zhang P, Zhang X, Cao N, et al. Curcumol potentiates celecoxib-induced growth inhibition and apoptosis in human non-small cell lung cancer. Oncotarget. 2017;8(70):115526–45.
55. Dempke W, Rie C, Grothey A, Schmoll HJ. Cyclooxygenase-2: a novel target for cancer chemotherapy? J Cancer Res Clin Oncol. 2001;127(7):411–7.
56. Chuang TY, Min J, Wu HL, McCrary C, Layman LC, Diamond MP, et al. Berberine Inhibits Uterine Leiomyoma Cell Proliferation via Downregulation of Cyclooxygenase 2 and Pituitary Tumor-Transforming Gene 1. Reprod Sci. 2017;24(7):1005–13.
57. Jung ID, Jeong YI, Lee CM, Noh KT, Jeong SK, Chun SH, et al. COX-2 and PGE2 signaling is essential for the regulation of IDO expression by curcumin in murine bone marrow-derived dendritic cells. Int Immunopharmacol. 2010;10(7):760–8.
58. Cianchi F, Cortesini C, Bechi P, Fantappie O, Messerini L, Vannacci A, et al. Up-regulation of cyclooxygenase 2 gene expression correlates with tumor angiogenesis in human colorectal cancer. Gastroenterology. 2001;121(6):1339–47.

Figures

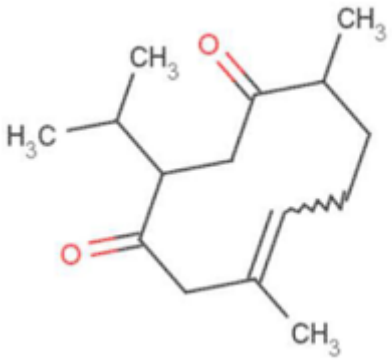

Figure 1

Chemical structure of curdione

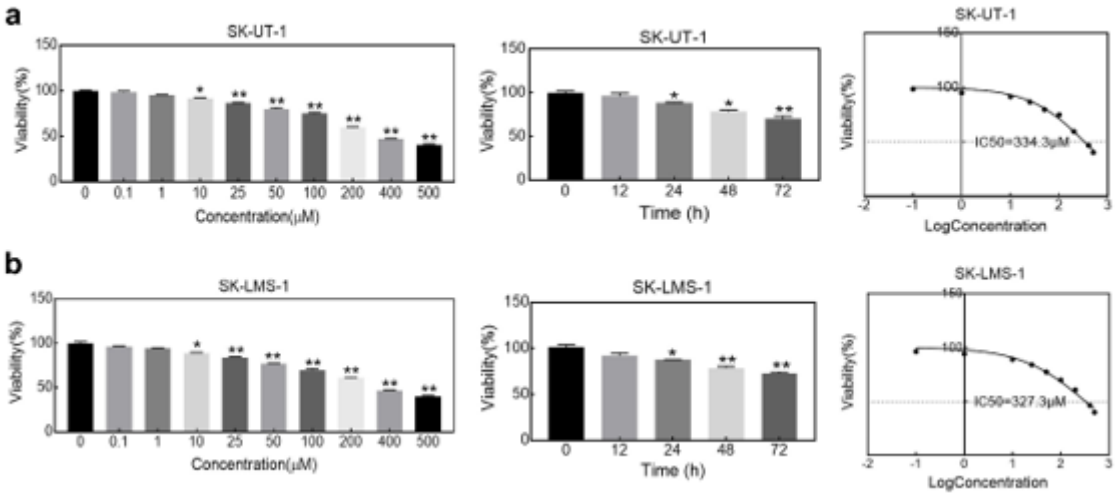

Figure 2

Curdione suppressed cell viability in human uterine leiomyosarcoma cells. Serum-starved uterine leiomyosarcoma cell lines (SK-UT-1(a) and SK-LMS-1(b)) were incubation with increasing concentrations of Curdione (0, 1, 10, 25, 50, 100, 200, 400, 500 μM) for 24 h, or with 100 μM Curdione for 12, 24, 48 and 72 h, the IC50 was calculated by non-linear regression using four-parameter logistic curves by GraphPad Prism7. Cell viability were detected by CCK8. All values are expressed the mean ± SD of three independent experiments. *P < 0.05, **P < 0.01 compared with control.

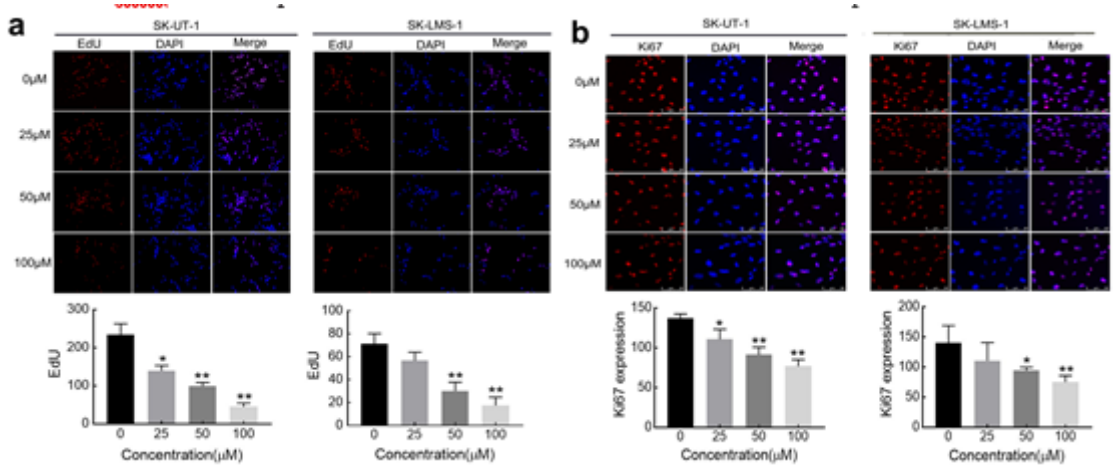

Figure 3

Anti-proliferation effect of curdione in SK-UT-1 and SK-LMS-1 cells. After treatment with curdione (0, 25, 50, 100 μM), the EdU retention assay (a) and ki67 protein expression (b) were measured by immune florescence. EdU-positive florescence images and the ki67 expression levels were analyzed by Image J, the results are shown in bar chart (*P□0.05, **P□0.01). Data presented as mean±SD of three independent experiments.

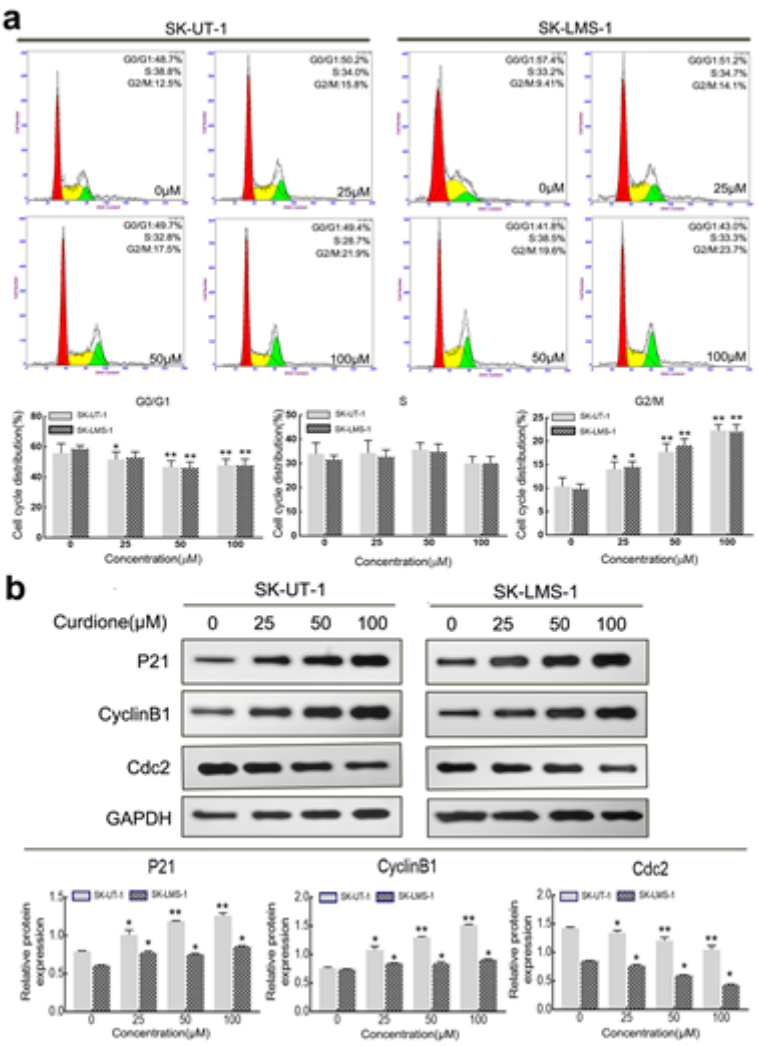

Figure 4

Curdion induces cell cycle arrest at G2/M phage in human uterine leiomyosarcoma cell lines. SK-UT-1 and SK-LMS-1 Cells were treated with 0, 25, 50 and 100 μM Curdione for 24 h, (a) the cell cycle distribution were analyzed by flow cytometry and (b) the cell cycle proteins P21, CylinB1, Cdc2 expression were detected by western blot. Histogram represented the statistical analysis of the cell cycle distribution ratio and proteins expression levels. All experiments performed three times, and the results present with means ± SD.*P < 0.05; **P < 0.01 compared with control.

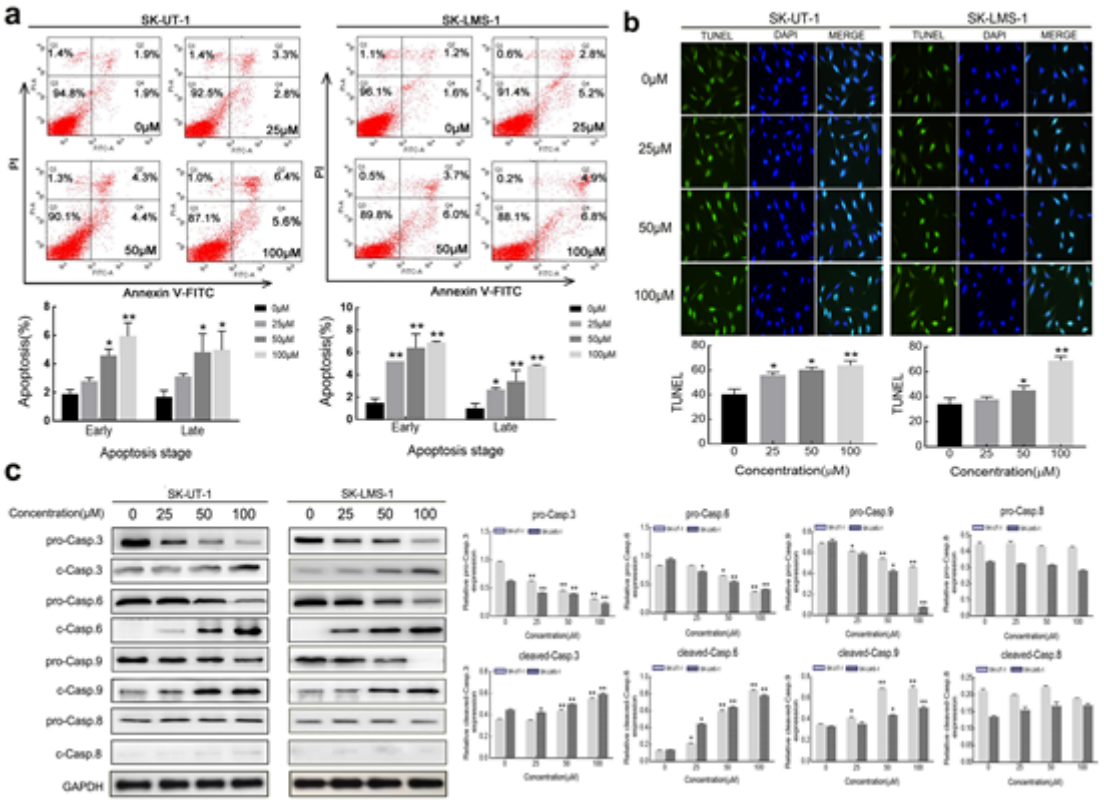

Figure 5

Curdione induces apoptosis in human uLMS cells and the apoptosis is mediate by caspases. SK-UT-1 and SK-LMS-1 Cells were treated with 0, 25, 50 and 100 μM Curdione for 24h (a) apoptotic ratio were analyzed with Annexin V-FITC/PI staining by flow cytometry. Both early and late apoptosis proportion were indicated by the histograms. (b) Apoptotic morphological changes were exhibited by TUNEL staining using fluorescent microscopy. Scale bars = 100 μm. The fluorescence intensity were analyzed and shown in the histogram. (c) Apoptotic associated proteins pro- and cleaved-caspase3, 6, 8, 9 expression levels of both cell lines were analyzed by western blot. Histogram represented the statistical analysis of the relative proteins expression level compared with GAPDH. All data were present with means ± SD of three independent experiments. *P < 0.05, **P < 0.01 compared with control.

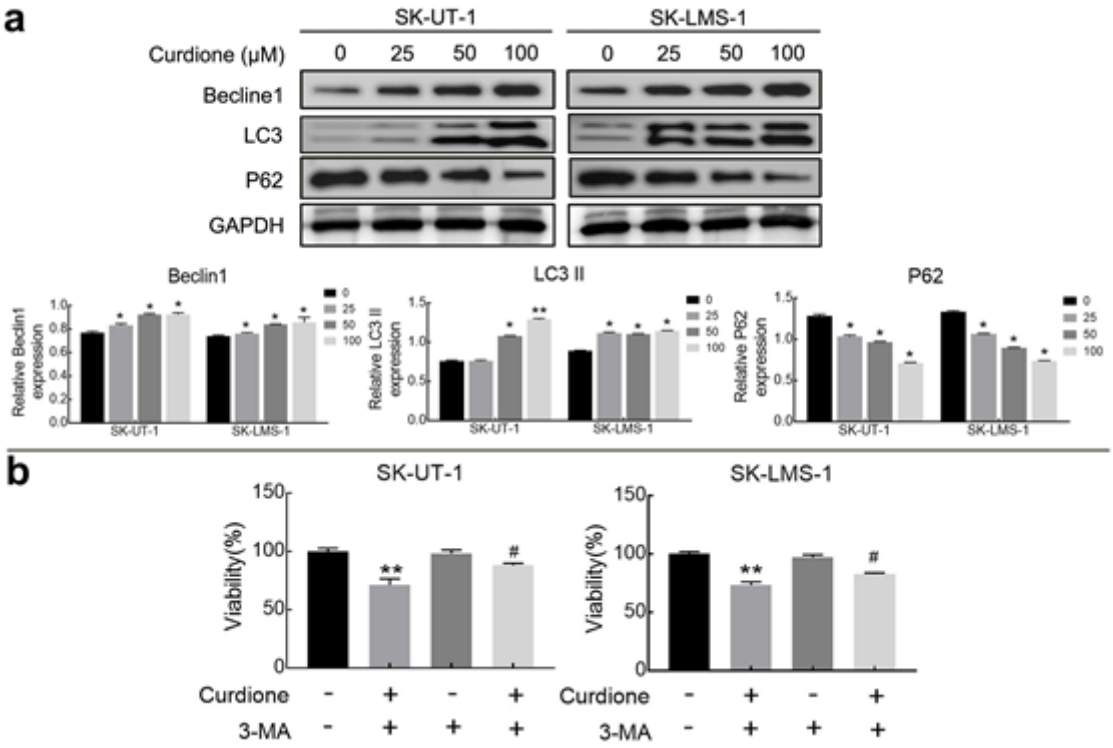

Figure 6

Curdione induces autophagy in human ULMS cells and the autophagy is pro-death. (a) After treatment with 0, 25, 50 and 100 μM Curdione for 24h，autophagy associated proteins Beclin1, LC3, P62 expression levels in both human uLMS cell lines were analyzed by western blot. (b) SK-UT-1 and SK-LMS-1 cells were treated with Curdione (100 μM) with 3-MA (2 mM) or not, CCK8 assay were performed to detected the cell viability. Histogram represented the statistical analysis data present with means ± SD of three independent experiments. *P < 0.05, **P < 0.01 compared with control; # P < 0.05; ## P < 0.01 compared with curdione alone group.

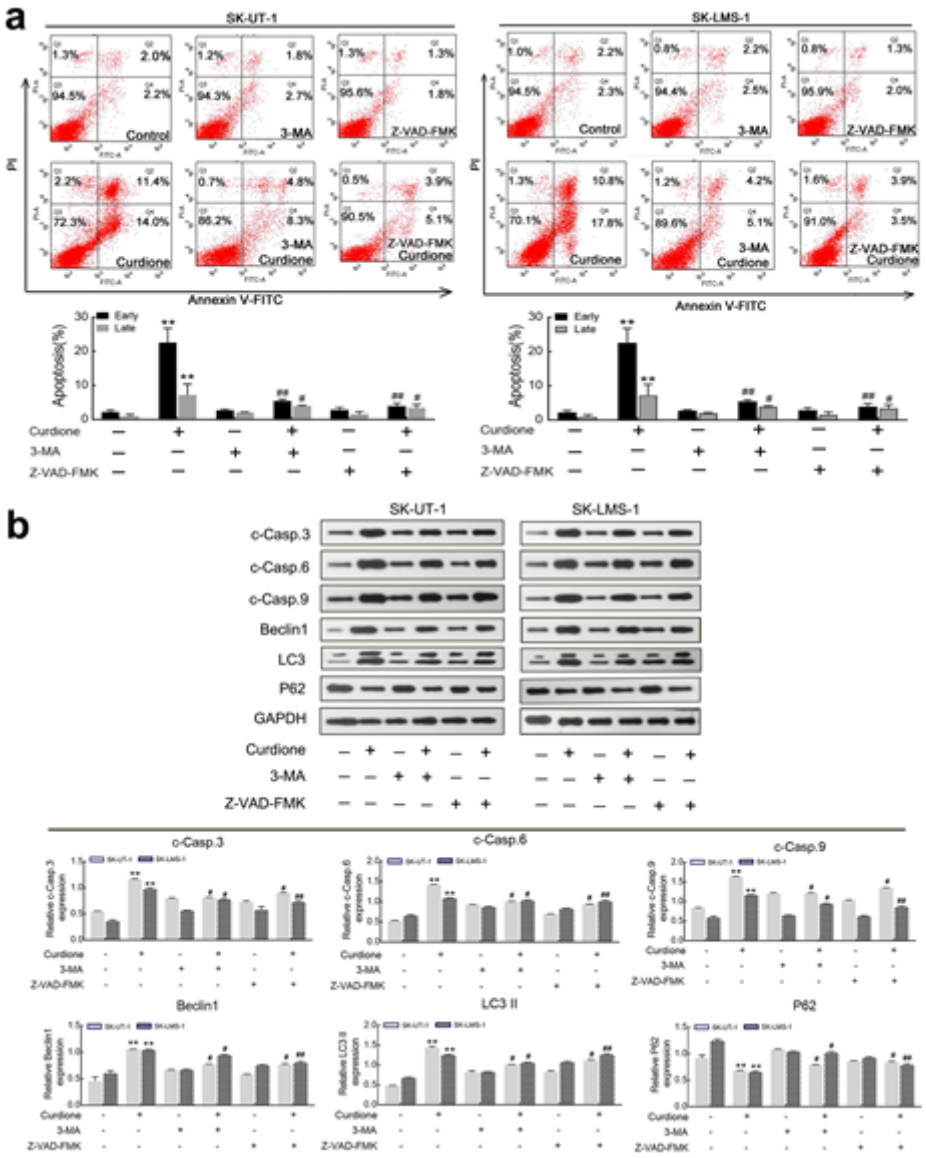

Figure 7

Curdione induced the crosstalk between apoptosis and autophagy. Inhibition of apoptosis alleviate Curdione-induced autophagy, while antagonism of autophagy attenuates curdione-induced apoptosis. SK-UT-1 and SK-LMS-1 cells were pretreated with Z-VAD-FMK (60 μM) or not and 3-MA (2 mM) or not for 2 h, following with Curdione (100 μM) for 24h. (a) The apoptosis was analyzed with Annexin V/PI staining by flow cytometry. (b) The protein expression levels of Beclin1, LC3B II, p62, and cleaved caspase-3, 6, 9 were determined by Western blot assays. The statistical analysis results of relative proteins expression levels compared with to GAPDH were shown in histogram. All date presented as the mean ± SD. *P < 0.05; **P < 0.01 compared with control; # P < 0.05; ## P < 0.01 compared with curdione alone group.

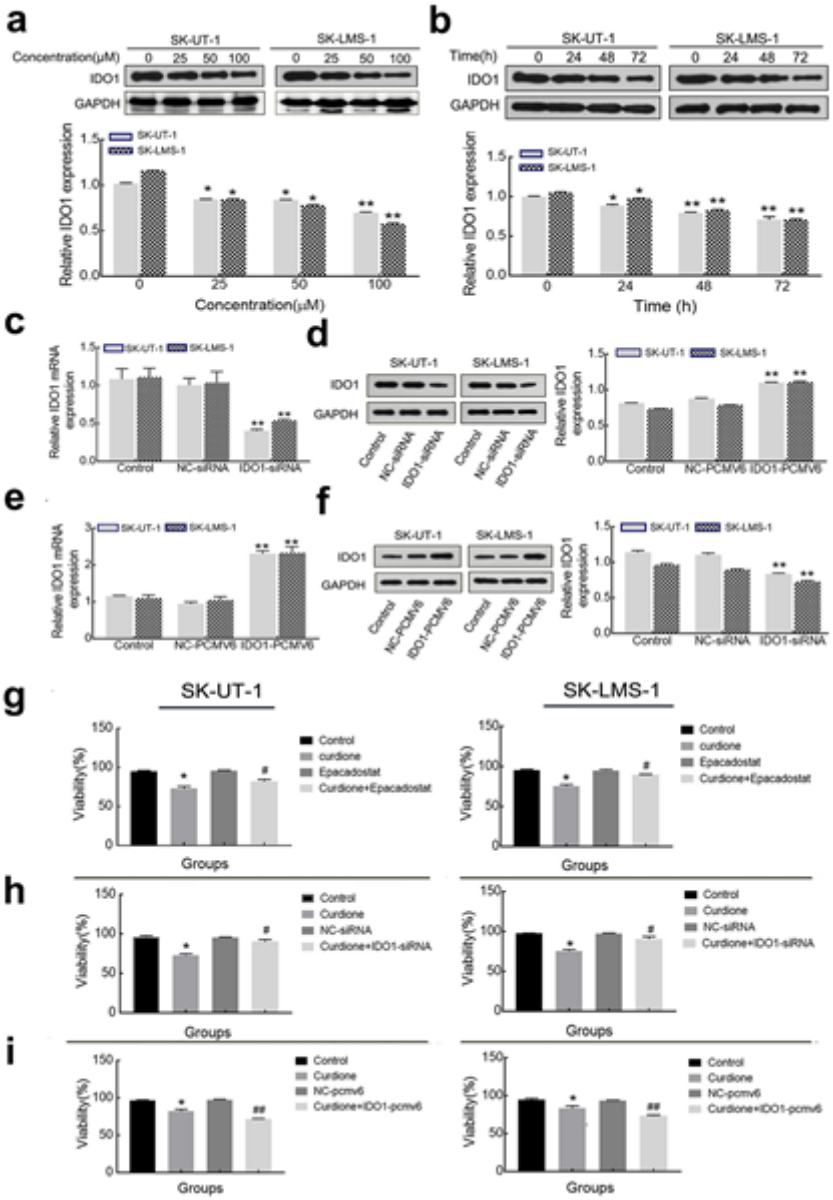

Figure 8

IDO1 mediated the anti-proliferation effect of curdione in uLMS cell lines. Cells were treated with 0, 25, 50 and 100 μM Curdione for 24 h, relative IDO1 protein expression levels were analyzed by western blot (a). Cells were treated with 100 μM curdione for 24, 48, 72 h, relative IDO1 protein expression levels were analyzed by western blot (b). To further explored whether the anti-proliferation effect of curdione in uLMS cells is mediate by IDO1. Cells were transiently transfected with IDO1 specific siRNA, IDO1 mRNA expression levels were confirmed by RT-PCR (c) and the protein expression levels were confirmed by western blot (d). Cells were transfected with IDO1 PCMV6 and confirmed mRNA expression by RT-PCR (e) and protein expression by western blot (f). Cells were pretreated with IDO1 inhibitor epacadostat (g) or transfected with IDO1 specific siRNA (h) or IDO1 PCMV6 (i), following with Curdione for 24 h, the cell viability were analyzed with CCK8 assay. Histogram represented the statistical analysis data from three independent trails and present with mean±SD. *P < 0.05; **P < 0.01 compared with control; #P < 0.05; ##P < 0.01 compared with curdione alone group.

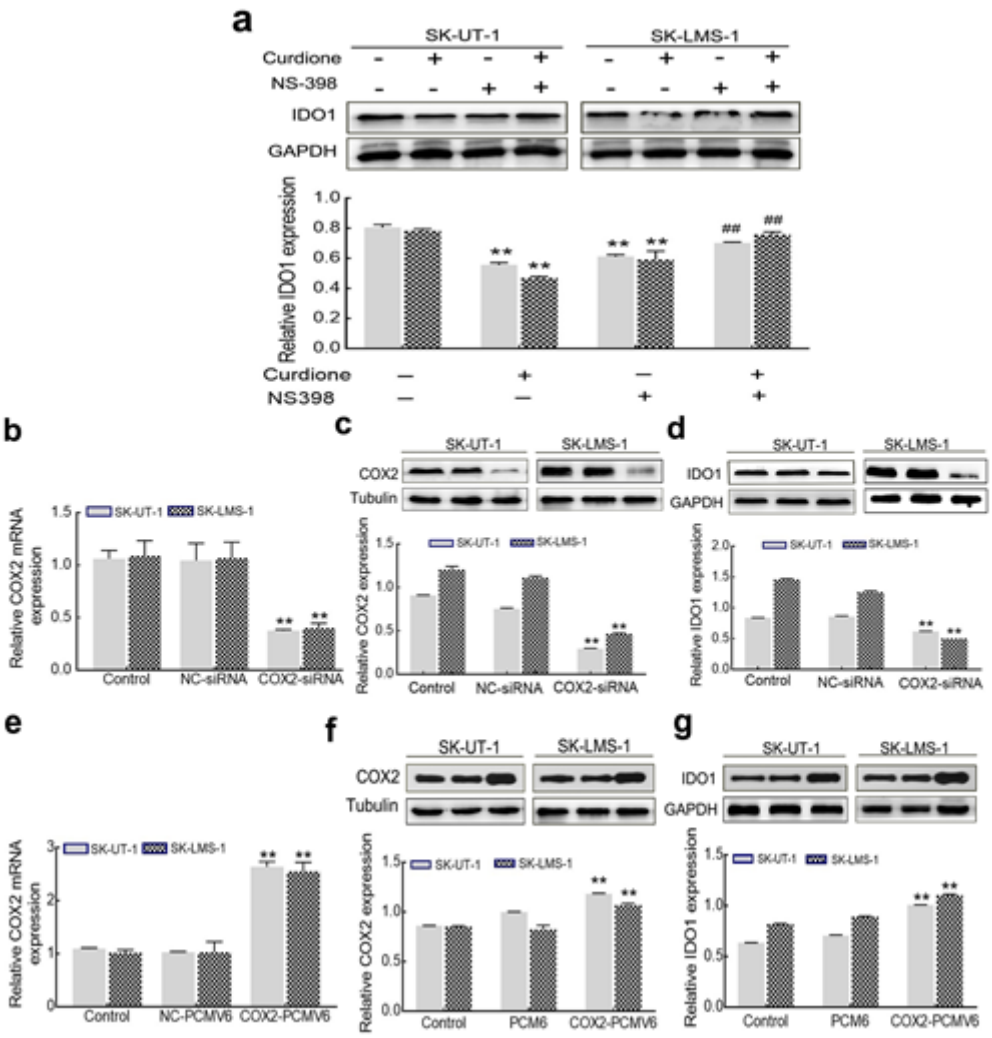

Figure 9

COX2 is essential for curdione-deduced IDO1 expression in human uterine leiomyosarcoma cell lines. SK-UT-1 and SK-LMS-1 cells were pre-treated with NS398 or not for 2 h and then incubated with 100 μM curdione for 24 h. IDO1 expression was determined using western blot and presented in histogram (a). After transiently transfected with specific COX2-siRNA or full-length cDNA of human COX2 (COX2-pCMV6). The COX2 mRNA and protein expression was confirmed by qRT-PCR analysis (b, e), and western blot analysis (c, f) respectively. After transfected with COX2-siRNA or COX2-pCMV6, cell were treated with curdione for 24 h, the IDO1 protein expression compared with GAPDH in SK-UT-1 and SK-LMS-1 cells were analyzed by western blot (d, g). All data are represent with mean±SD and present in histogram. All experiments performed triplicate. *P < 0.05; **P < 0.01 compared with control; #P < 0.05, ##P < 0.01 compared with curdione alone group.

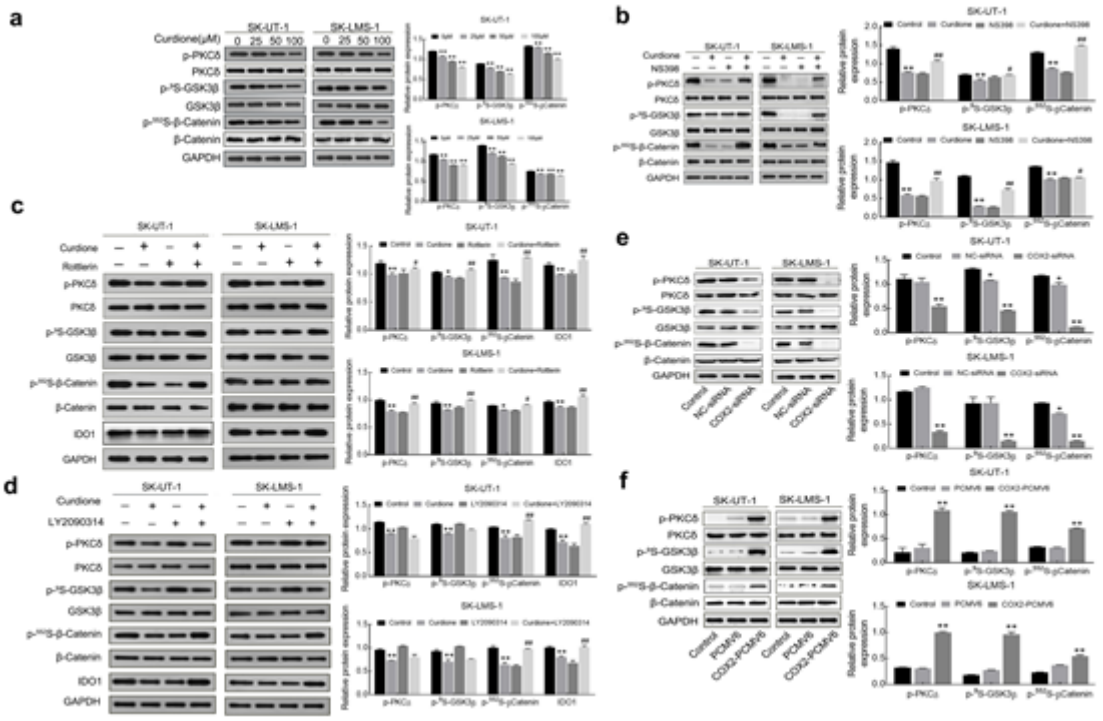

Figure 10

Curdione induces deduces IDO1 expression through COX2 mediate PKCδ/GSK3β/β-catenin pathway in uLMS cells. SK-UT-1 and SK-LMS-1 cells were incubated with 0, 25, 50, 100 μM curdione for 24 h (a), or pretreatment with NS398 (b) or rottlerin (c) or LY2090314 (d) for 2 h, and then incubated with 100 μM curdione for 24 h. Cells were transfected with either COX2-siRNA (e) or COX2-pCMV6 (f), and then, incubated with 100 μM curdione for 24 h. The PKCδ, GSK3β (ser9), β-Catenin (ser552) phosphorylation and IDO1 expression were evaluated by western blot analysis. The histograms represent the relative expression of phospho-PKCδ (p-PKCδ) or phospho-GSK3β (ser9) or β-Catenin (ser552) compared with PKCδ or GSK3β (ser9) or β-Catenin (ser552), respectively. All data are present with mean±SD in histogram. All experiments performed triplicate. *P < 0.05, **P < 0.01 compared with control; #P < 0.05, ##P < 0.01 compared with curdione alone group.

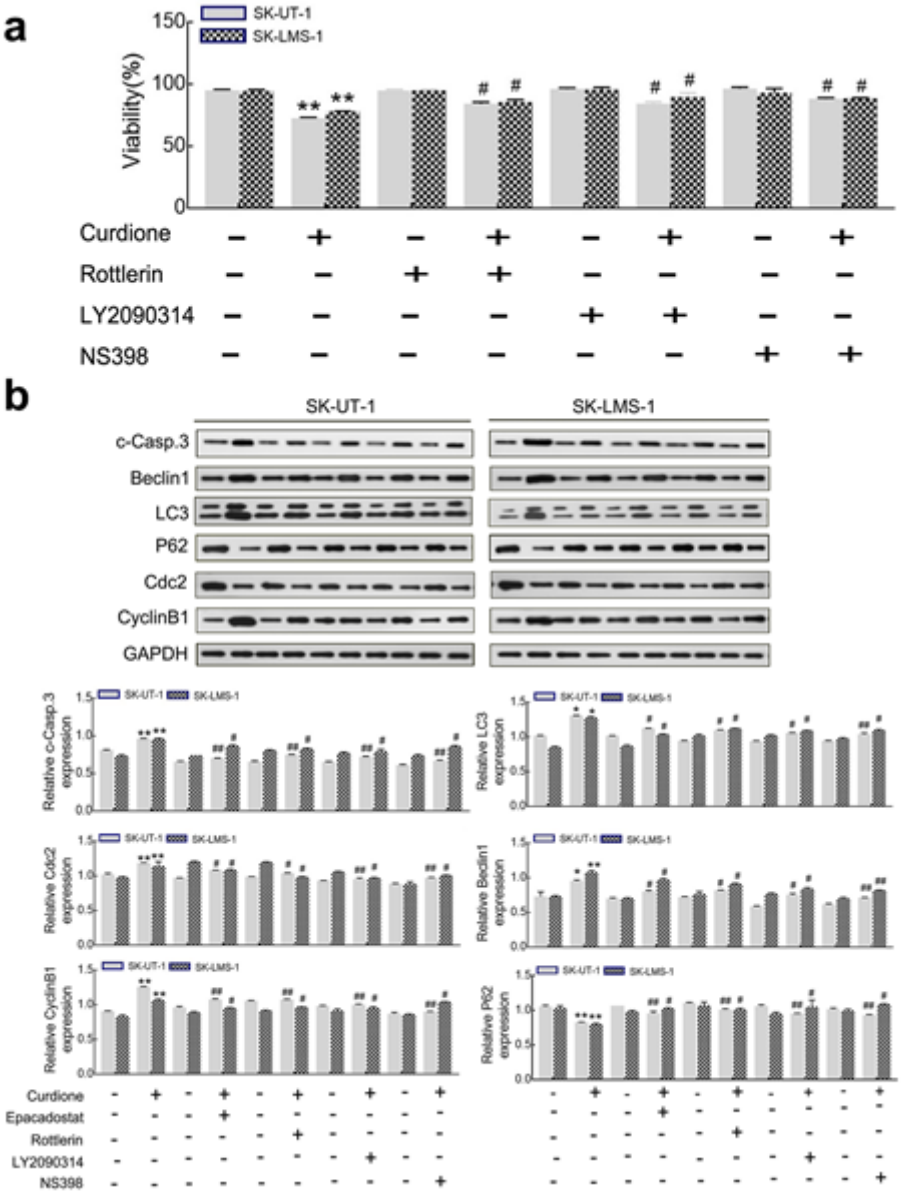

Figure 11

Curdione inhibited the proliferation effect of human uterine leiomyosarcoma by inducing apoptosis, autophagy and cell cycle arrest in G2/M. Starved SK-UT-1 and SK-LMS-1 cells were pretreated with Epacadostat, Rottlerin, LY2090314 or NS398 for 2 h followed with 100 μM Curdione for 24 h, the cell viability was determined by CCK8 assay (a). The caspases related proteins cleaved-caspase 3, 6, 9; autophagy marker Beclin1, LC3, P62; and cell cycle related proteins CylinB1 and Cdc2 were analyzed by western blot (b). All data are represent with mean±SD and present in histogram. All experiments performed triple. *P < 0.05; **P < 0.01 compared with control; #P < 0.05, ##P < 0.01 compared with curdione alone group.

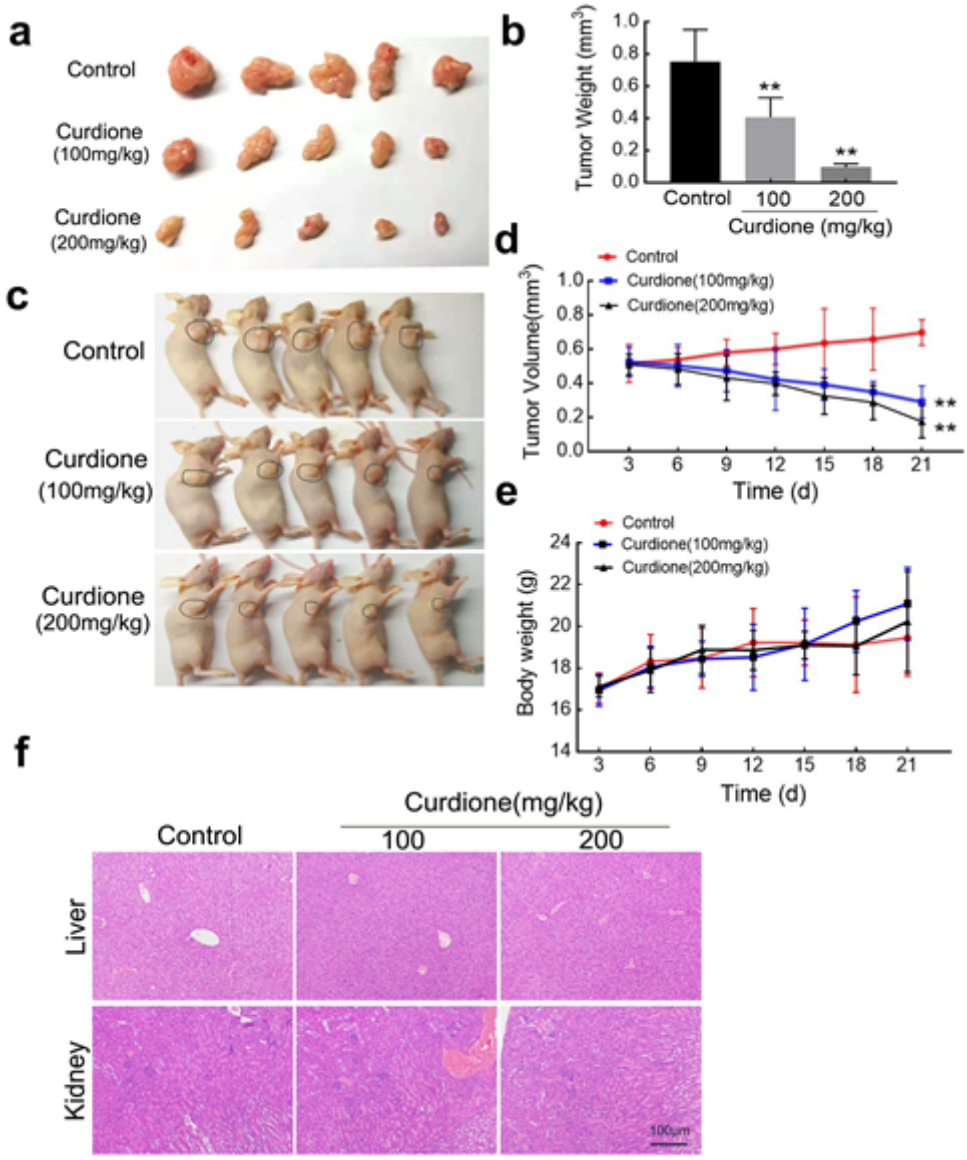

Figure 12

Anti-proliferation effect of curdione in SK-UT-1 xenograft tumor models. BALB/c nude mice were subcutaneously inoculated with SK-UT-1 cells (1x107 /mouse) in the right flank. When volume of tumor reached around 50 mm3, mice were administration of solvent or curdione (100 and 200 μg/kg/d) intraperitoneal. 21 days later, all mice were executed. Representative images were taken photos (a, c), tumor weight (b) were determined and recorded. Tumor volume (d) and body weight (e) were measured every three days. (f) The histological immunohistochemical in tumor tissues was assessed by the H&E staining. Scale bars = 100 μm. Apoptosis and autophagy associate proteins, PKCδ, GSK3β and β-cantein and there phosphorylation forms in tumor tissues were analyzed by western blot. All data are represent with mean±SD and present in histogram. *P < 0.05, **P < 0.01 compared with control.

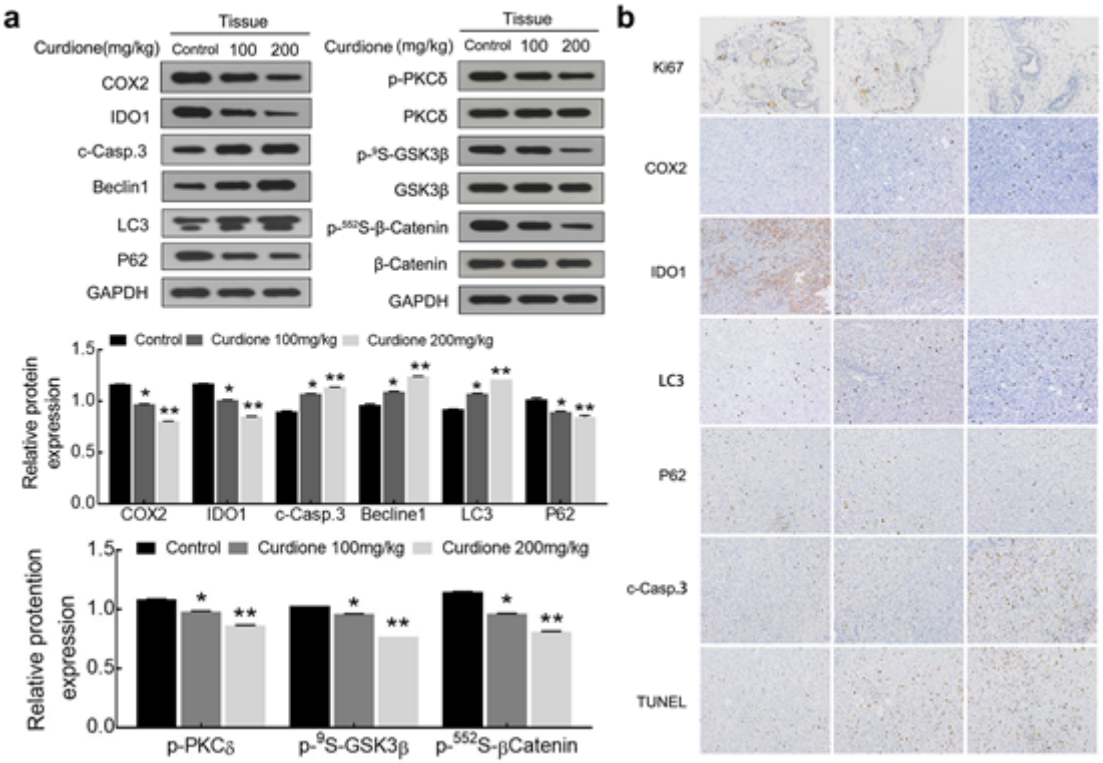

Figure 13

Curdione induces apoptosis and autophagy in SK-UT-1 xenograft tumor models. (a) The protein expression levels of COX2, IDO1, cleaved caspase-3, beclin1 LC3B II, p62, p-PKCδ/PKCδ, p-GSK3β/GSK3β and p-β catenin/β catenin were detected by western blot analysis, the statistical analysis of the relative expression level presented in histogram. (b) The expression levels of Ki67, COX2, IDO1, cleaved caspase-3, LC3, p62 proteins were determined by immunohistochemistry. Scale bars = 100 μm. All statistical analysis data are present with mean±SD in histogram. *P < 0.05, **P < 0.01 compared with control.